ACS OMEGA

http://pubs.acs.org/journal/acsodf

Article

Enthalpies of Immersion in Caffeine and Glyphosate Aqueous Solutions of SBA-15 and Amino-Functionalized SBA-15

Paola Rodríguez-Estupiñan, Yaned Milena Correa-Navarro, Diana P. Vargas, Liliana Giraldo, and Juan Carlos Moreno-Piraján*

Cite This: *ACS Omega* 2021, 6, 21339−21349

Read Online

ACCESS | Metrics & More | Article Recommendations

ABSTRACT: Mesostructured silica SBA-15 and amino-functionalized silica SBA-15-NH_2 were synthesized, and then, characterization, adsorption capacity, and immersion enthalpies in caffeine and glyphosate on SBA-15 and SBA-15-NH_2 were evaluated. The enthalpy parameter was determined using a local construction Tian-type heat conduction calorimeter. Calorimetric studies in caffeine solutions exhibit negative enthalpy values; exothermic process characteristics for SBA-15 were between −13.90 and −194.06 J g^{-1} and those for SBA-15-NH_2 were between −7.22 and −60.34 J g^{-1}, and the adsorption capacity of caffeine was better in SBA-15 than that in SBA-15-NH_2. In contrast, the enthalpies of immersion in glyphosate solutions were −5.06 to −56.2 J g^{-1} and the immersion of SBA-15-NH_2 in each solution generated enthalpy values of −9.06 to −41.2 J g^{-1}, but the adsorption capacity of glyphosate was better in the amino-functionalized SBA-15. The results show that functionalization of SBA-15 produced differences in physicochemical characteristics of solids, since energy and affinity for the calorimetric liquids are related to the surface properties of solids as well as the chemical nature of the target molecule, immersion enthalpy, was different.

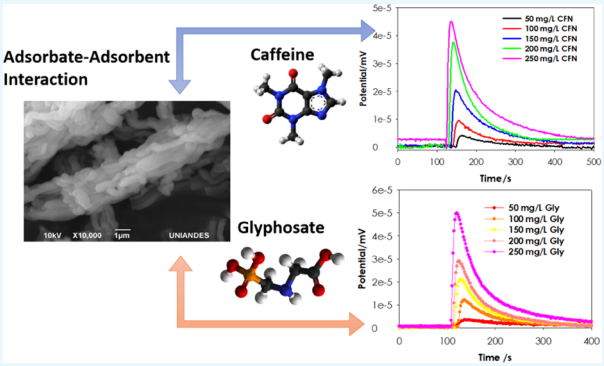

1. INTRODUCTION

Water pollution and poor sanitation undermine progress in other areas of development (UNICEF), so the effective water treatment and sanitation are a challenge today to meet the growing demand of the world population.[1−3] A group of pollutant compounds that have been detected in superficial water, groundwater, and even in drinking water at low concentrations and that are not regulated despite the proven adverse effect they have on different organisms have been called emerging contaminants (EC).[4,5] These types of contaminants can originate from sources such as household chemicals, agrochemicals, and pharmaceutical products. Here, we have selected two organic pollutant representatives of these groups and are currently being studied for their recurrence in surface waters. Caffeine is a central nervous system stimulant of high human consumption, mainly in energy drinks and as adjuvant medicine is an EC. This molecule when ingested by humans is metabolized or not into smaller molecules that are frequently detected in water tributaries.[6] Although glyphosate (*N*-phosphonomethylglycine) is the most widely used pesticide around the world, this is a polar molecule with high water solubility, used as the active ingredient with herbicidal action of commercially available formulations of pesticides (Roundup). Glyphosate is a nonselective post-emergent type of herbicide; its herbicidal action is due to its ability to inhibit the shikimic acid pathway in plant metabolism.[4,7]

To remove pollutants of water samples, different processes are employed. However, conventional treatments are not effective and so harmful molecules remain in aquifers and cause deterioration in ecosystems. Hence, it is necessary to combine efforts in finding techniques that allow the total removal of EC from the aquifers. Among the options that are being used, the adsorption processes with different types of adsorbents such as active carbon, biochar, metal organic framework, mesostructured silica, and others can be found.[1,3,8]

The discovery of mesostructured silicas led to the opening of a new field of research in the design of porous solids. In general, mesostructured silicas are synthesized from the mixture of a silicon source and a structuring agent that confers an organized mesoporous structure, high surface area, and tunable pore size as well as a heterogeneous surface composed of both hydrophobic sites—siloxane groups, and polar sites—

Received: March 24, 2021
Accepted: June 25, 2021
Published: August 12, 2021

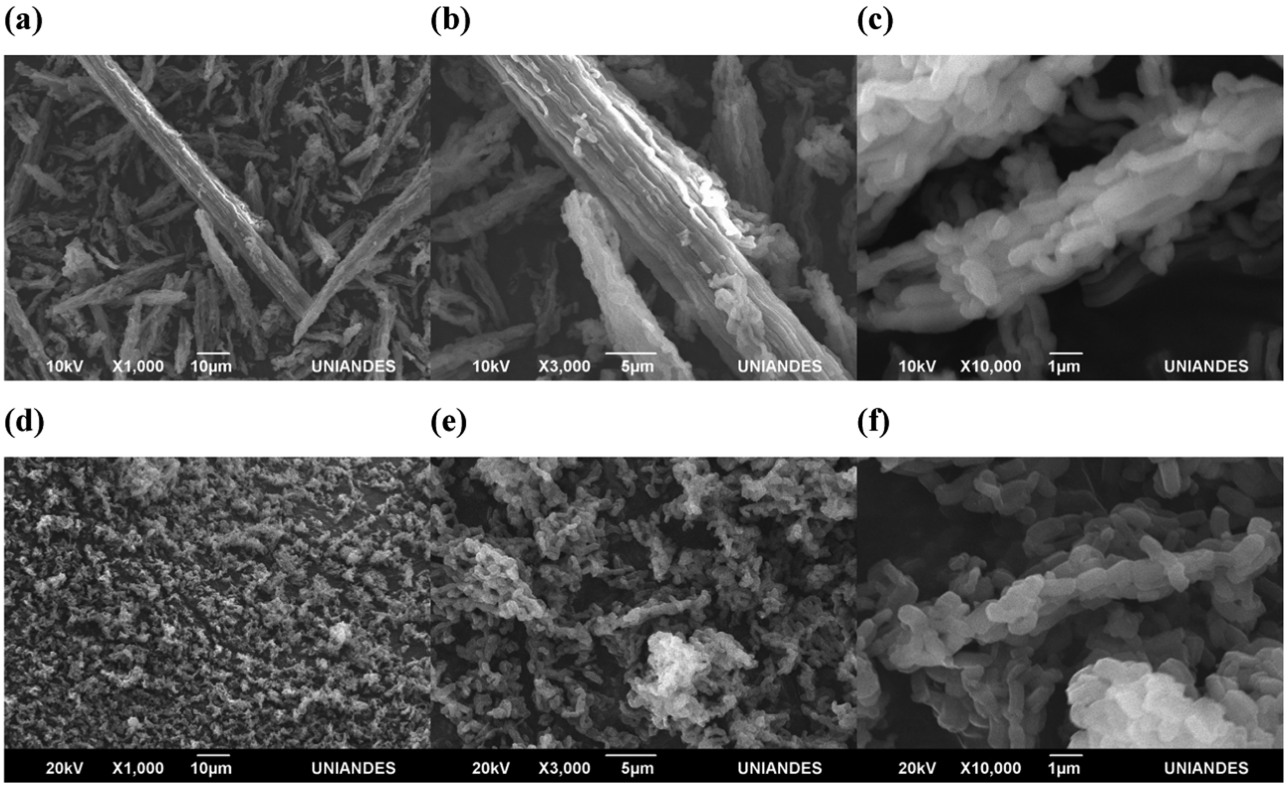

Figure 1. SEM micrograph at different magnifications of the (a−c) SBA-15 and (d−f) SBA-15-NH2 samples.

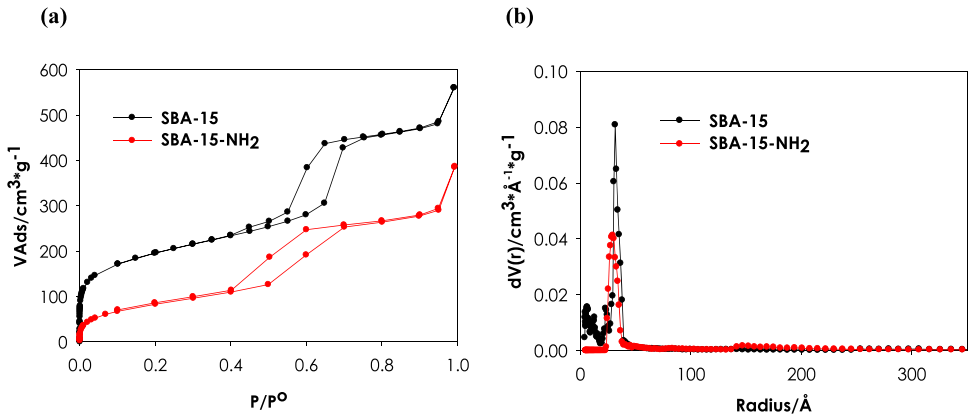

Figure 2. (a) N_2 adsorption−desorption isotherms and (b) pore size distributions (PSD) by quenched solid density functional theory (QSDFT) of SBA-15 and amino-modified solid.

silanol groups.[9−11] Some arguments against the use of this type of inorganic template material are related to the production cost and scalability.[9−12] In this sense, production optimization and lower cost techniques have been explored, including use of alternative silicon sources such as rice husk[13,14] or coal fly ash[15] and washing methods with environmentally friendly solvents to remove the template.[12] Additionally, the ability of SBA-15 to host a large series of functional groups by methods of cocondensation, isomorphic replacement, or grafting leads it to be a promising porous solid[10] that opens a tremendously valuable possibility of developing solids with very specific characteristics, for industrial applications related to adsorption processes[16,17] and membrane separation,[18,19] in pharmaceutical applications like drug delivery,[20,21] biosensing,[22,23] and for catalysis.[24,25]

As mentioned above, due to its textural and chemical properties, SBA-15 has been used for the adsorption of different types of molecules. SBA-15 was also demonstrated to be versatile due to its capacity to modify the surface chemistry by anchoring molecules. In this way, the type of interactions can be designed that are established with the target molecule; the interaction can be site-specific, nonspecific, or both.[10,26,27] Immersion calorimetry has proven to be a valuable tool for studying adsorbate−adsorbent interactions and is sensitive to changes in the surface chemistry of the adsorbent.[28] Accordingly, the objective of the present study is to characterize the liquid−solid interactions by determining the enthalpies for immersion in water and aqueous solutions of caffeine and glyphosate; the adsorption capacity of these molecules on SBA-15 and its modification by the anchoring of amine functional groups (SBA-15-NH_2) was also determined.

https://doi.org/10.1021/acsomega.1c01588
ACS Omega 2021, 6, 21339−21349

2. RESULTS AND DISCUSSION

2.1. Physicochemical Characterization. The sample morphology was studied by scanning electron microscopy (SEM). Figure 1 shows the micrographs of SBA-15 at different magnifications (Figure 1c); the micrographs of SBA-15 that was subjected to the process of anchoring the molecule (3-aminopropyl)triethoxysilane (APTES) in ethanol are also presented. The SEM analysis showed the typical SEM images for SBA-15, which consisted of arrangements of rod-shaped particles attached with a uniform grain size of approximately 1 μm, resembling the structure of a rope. In addition, morphological changes of functionalized SBA-15 were not clear although changes in the grain size after the functionalization process could be observed.[28]

On the other hand, the N_2 adsorption−desorption isotherms of SBA-15 and SBA-15-NH_2 are presented in Figure 2. The isotherms were classified as type IV(a), attributed to mesoporous solids, with cylindrical pores in hexagonal arrangements.[29] A reduction in the capacity of nitrogen adsorption was evidenced for the functionalized sample, SBA-15-NH_2. At relatively pressures higher than 0.1 in the isotherm, a change in the behavior in nitrogen adsorption could be observed, which increased gradually; at this pressure, a monolayer of nitrogen molecules in the pores was formed. Also, SBA-15 and SBA-15-NH_2 show a hysteresis loop on a range of relative pressures (0.4−0.80). The changes in the slopes of the adsorption data are associated with the presence of micropores in the walls of SBA-15, which was associated to the capillarity mechanism adsorption process and the condensation of N_2 into bigger pores. The textural parameters obtained for the solids SBA-15 and SBA-15-NH_2 are summarized in Table 1.[30,31]

Table 1. Textural Parameters Evaluated from the N_2 Adsorption−Desorption Isotherms

samples	SBA-15	SBA-15-NH_2
S_{BET} (m^2 g^{-1})	693	302
V_{DR} (cm^3 g^{-1})	0.25	0.09
average half-pore width (Å) DR	8.03	10.4
E_0 (kJ mol^{-1})	12.5	16.2
half-pore width (mode) (Å) DFT model	31.6	29.4
V_{BJH} (cm^3 g^{-1})	0.87	0.58

SBA-15 had a specific surface area (S_{BET}) of 693 m^2 g^{-1}; after the functionalization process, this parameter decreased to 302 m^2 g^{-1}. The same behavior was observed for volume pore evaluated by the Dubinin−Radushkevich (DR) and Barrett−Joyner−Halenda (BJH) methods. There was a decrease in these parameters because of the anchoring of APTES molecules on the pore walls and over pore openings; the APTES molecule occupied the previously available sites, and the change in the adsorption capacity on the micropores and mesopores could be associated with the existence of a steric effect. The most probable pore size of SBA-15 according to the NLDTF model for cylindrical pore was 31.6 Å, which changed to 19.4 Å for SBA-15-NH_2.[32−3432−34]

On the other hand, infrared spectroscopy showed the changes in the surface after the functionalization process. The infrared spectra of the mesostructured silica are shown in Figure 3. Characteristic bands for SBA-15 were observed between 460 and 1090 cm^{-1}, related to silica condensed networks and were associated to the stretching vibration of Si−O−Si. Also, the band located at 3400 cm^{-1} was associated to the OH stretching of silanol groups. This band decreased in SBA-15-NH_2, indicating that the 3-aminopropyltriethoxysilane molecule effectively interacted with OH groups of SBA-15.[35,36] Two bands observed were evidence of a functionalization process with APTES: (i) the band located at 1600 cm^{-1}, indicating bending vibrations of the NH_2 groups in a primary amine and (ii) the band located between 2870 and 2940 cm^{-1} related to the symmetric and asymmetric stretching vibrations of the C−H of the propyl chain of the group anchoring.

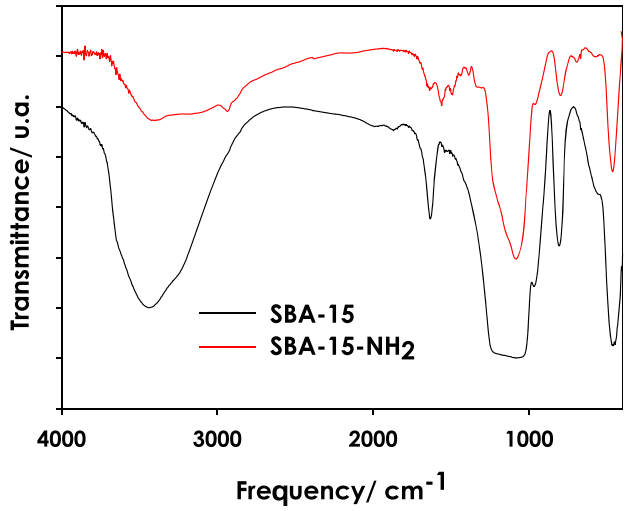

Figure 3. Fourier transform infrared spectroscopy (FTIR) of SBA-15 and SBA-15-NH_2.

The thermal stability of the solids prepared in this work was evaluated by thermogravimetric analysis (TGA). Figure 4a presents the individual thermograms for SBA-15 and its modifications; from the weight loss derivatives, there were different temperature ranges where the loss of mass was associated to different processes that occur on the surface of SBA-15. At least three characteristic regions were observed for the modified silica and only two for SBA-15 (see Figure 4b). In the temperature range between 30 and 200 °C, desorption of water molecules and solvents such as ethanol (from the functionalization process) is presented. The desorption of water molecules is observed up to 240 °C due to the formation of stronger interactions with the surface complexes by means of hydrogen bonds.

For the amino-functionalized solid, the temperature range located between 125 and 600 °C was related to the thermal decomposition of the organic complexes anchored to the surface of SBA-15 and residues of the structuring agent, and the total loss of weight of the modified solid was approximately 15%. Also, for SBA-15 in the region between 300 and 700 °C, the condensation of the silanol groups to siloxane groups is presented, reflecting a change in the steric interactions between the silanol groups.[35,37] From the thermogravimetric data, the amount of silanol groups can be evaluated according to the following equations[35]

$$n_{OH} = 2n_{H_2O} = \frac{(W_{T_i} - W_{T_f})}{100 * M_{H_2O}} = \frac{\text{mmol}}{\text{g}} \quad (1)$$

where W_{T_i} and W_{T_f} correspond to the percentage of weight loss in an initial and final temperature range, respectively, M_{H_2O} is the molecular weight of water, and the temperature ranges that

https://doi.org/10.1021/acsomega.1c01588
ACS Omega 2021, 6, 21339−21349

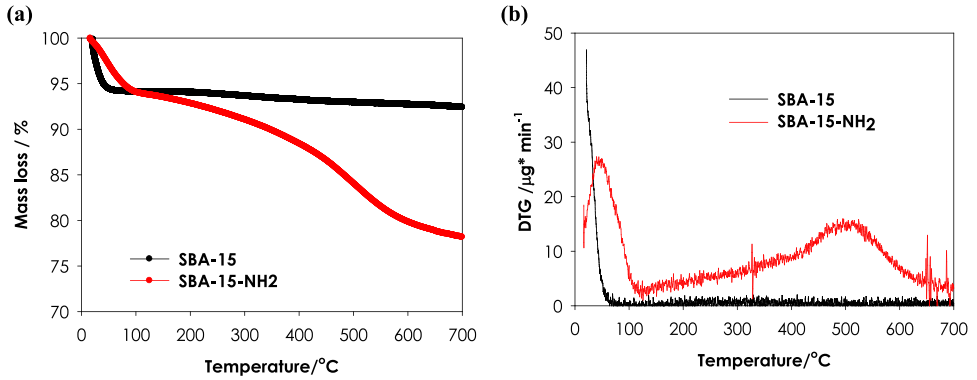

Figure 4. (a) TGA of SBA-145 and SBA-15-NH_2, (b) derivative thermogravimetry (DTG) of SBA-145 and SBA-15-NH_2.

have been established are 30−200 and 200−800 °C. The number of water molecules and OH groups per nm^2 is obtained from eq 2

$$N_{OH\cdot H_2O}\left(\frac{\text{molecules}}{nm^2}\right) = \frac{n\left(\frac{\text{mmol}}{g}\right) * \frac{1.0\times10^{-3}\ \text{mol}}{1\ \text{mmol}} * N_A\left(\frac{6.023\times10^{23}\ \text{molecules}}{1\ \text{mol}}\right)}{A_{BET}\left(\frac{m^2}{g}\right) * \frac{1.0\times10^{18}\ nm^2}{1\ m^2}} \quad (2)$$

where n is the number of water and OH groups in mmol g^{-1}; NA is the Avogadro number, and A_{BET} is the apparent surface area of the solid.

According to the values shown molecules in the study intervals in Table 2, the number of OH groups per nm^2 obtained for SBA-15 is 3.85, which is in accordance with the values reported in the literature; these data are not recorded in the table for solid SBA-15-NH_2 due to the decomposition of APTES molecules in the study intervals and that interfered with the calculation.

Table 2. Hydroxyl Group Content in SBA-15

	physically adsorbed water content			hydroxyl group content		
sample	W_{H_2O} (%)	n_{H_2O}	N_{H_2O}	W_{OH} (%)	n_{OH}	N_{OH}
SBA-15	4.06	2.26	2.05	3.82	4.24	3.85

2.2. Calorimetric and Equilibrium Characterization of Caffeine and Glyphosate Adsorption. As mentioned previously, the main objective of this work is to evaluate the performance of mesostructured silicas in the removal of emerging contaminants such as caffeine and glyphosate. For this, the calorimetric effect of the immersion of silicas in solutions of known concentrations of caffeine and glyphosate as well as the adsorption equilibrium were studied.

The samples were characterized by immersion enthalpy values in water, caffeine, and glyphosate solutions to evaluate the interaction between surface silica−solvent and surface silica−target molecules. Immersion enthalpy is a thermodynamic parameter that can be correlated to the pore structure and surface chemistry nature of the adsorbent. Figures 5a,b and 6a,b show the curves obtained for SBA-15 and SBA-15-NH_2 in caffeine and glyphosate solutions at different concentrations, respectively. The heat exchanged in the immersion process is proportional to the area under the curve of the potential versus time.

The immersion enthalpies in water and different solutions are summarized in Table 3. As mentioned above, the enthalpy of immersion varies with the type of interaction that is established between the solid and the solvent and the solid and the target molecule. Thus, a higher enthalpy of immersion in water is an indication of the hydrophilic nature of the solid, as in the case of SBA-15, whose surface interacts with the solvent molecules through surface silanol groups, while a decrease is observed in the enthalpy of immersion in water for the solid SBA-15-NH_2; this is due to the binding of the aminosilane molecules that have joined the silanol groups as well as the

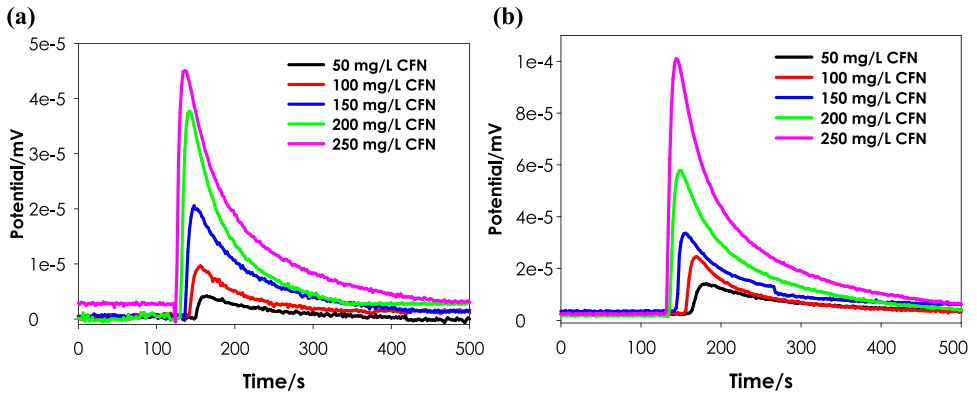

Figure 5. Potentiograms obtained from the immersion of (a) SBA-15 and (b) SBA-15-NH_2 in caffeine solution at different concentrations (50−250 mg L^{-1}).

https://doi.org/10.1021/acsomega.1c01588
ACS Omega 2021, 6, 21339−21349

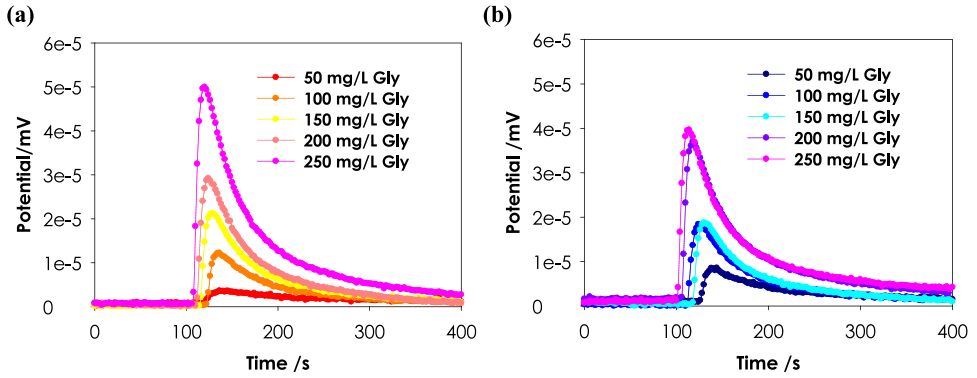

Figure 6. Potentiograms obtained from the immersion of (a) SBA-15 and (b) SBA-15-NH_2 in glyphosate solution of different concentrations (50–250 mg L^{-1}).

Table 3. Immersion Enthalpies of SBA-15 and SBA-15-NH_2 in Water and Caffeine and Glyphosate Solution of Different Concentrations

molecule	caffeine		glyphosate	
sample liquid	$-\Delta H$ Imm SBA-15 (J g^{-1})	$-\Delta H$ Imm SBA-15-NH_2 (J g^{-1})	$-\Delta H$ Imm SBA-15 (J g^{-1})	$-\Delta H$ Imm SBA-15-NH_2 (J g^{-1})
water	127.3 ± 1.61	49.7 ± 0.67	127.3 ± 1.61	49.7 ± 0.67
50 mg L^{-1}	13.9 ± 1.54	1.06 ± 0.24	5.06 ± 1.54	9.06 ± 0.24
100 mg L^{-1}	27.5 ± 2.18	13.6 ± 1.36	13.1± 2.18	22.6 ± 1.36
150 mg L^{-1}	89.1 ± 3.56	26.9 ± 1.96	30.2 ± 3.56	24.8 ± 1.96
200 mg L^{-1}	101.2 ± 3.84	32.9 ± 1.88	35.6 ± 3.84	36.7 ± 1.88
250 mg L^{-1}	194.1 ± 4.64	43.7 ± 2.56	56.2 ± 4.64	41.2 ± 2.56

hydrophobic effect of the propyl chains of APTES. The difference of the enthalpy of immersion in water is an indication of the change in the surface chemistry of solids, a product of the anchoring of the APTES molecule. In the case of SBA-15, the enthalpy effect is due to the formation of hydrogen bonds between the water molecules and the silanol groups; however, the enthalpy of water immersion decreased in SBA-15-NH_2 by reducing the accessible silanol groups for polar interactions due to a screening effect by APTES molecules anchored to the surface of SBA-15 and the presence of carbon chains and the hydrophobic effect that this implied.[26,38,39]

The enthalpy contributions of the surface sites give rise to specific interactions if the study molecule has a high dipole moment and/or functional groups capable of interacting with the surface; therefore, the released energy can be related to the formation specific intermolecular interactions of these specific interactions such as hydrogen bonds between the sites and the particles adsorbed on the surface of the solid. Caffeine and glyphosate have different moieties that can establish different interactions with functional groups on the silica surfaces. Caffeine (Figure 7a) is an amphiphilic weak-basic purine base, and imidazole and carbonyl groups in its structure can establish specific intermolecular interactions with hydroxyl groups of silica, while the electrons localized on nitrogen atoms of amine

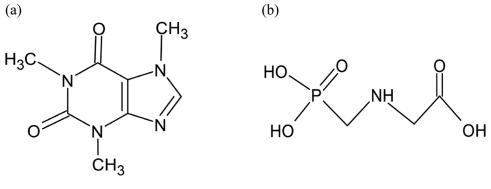

Figure 7. Chemical structures of (a) caffeine and (b) glyphosate.

and imine groups such as aromatic rings interact with oxygen atoms.[40,41] On the other hand, glyphosate may form chemical interaction via binding to the highly reactive phosphonomethyl group; the protonated amine and carboxymethyl groups may interact with hydrogen bonds and electrostatic interactions can be favored with the deprotonation of the molecule due to its polyprotic nature, with pK_a values of 2.6, 5.6, and 10.6 for phosphonomethyl, carboxymethyl, and amine groups, respectively.[42]

Calorimetric studies in the caffeine solution showed that the immersion of SBA-15 in each solution yielded enthalpy values of −13.9 to −194.1 J g^{-1} and the immersion of SBA-15-NH_2 in each solution yielded enthalpy values of −7.22 to −60.3 J g^{-1} (see Table 3). However, for the glyphosate solutions of SBA-15, each solution yielded enthalpy values of −5.06 to −56.2 J g^{-1} and the immersion of SBA-15-NH_2 in each solution yielded enthalpy values of −9.06 to −41.2 J g^{-1}. The results show that the functionalization of SBA-15 produced differences in characteristics of solids; since energy and affinity for the solvent and aqueous solutions are related to the solid surface properties, immersion enthalpies were different. It is important to note that the enthalpy effects for the SBA-15-NH_2 sample are lower than SBA-15, and this may be related to the decrease in textural parameters because the amino groups can be located at the edges of the pore openings.[39]

Figure 8a,b shows the enthalpy values as a function of initial concentrations of solutions. As mentioned before, immersion enthalpy is an integral heat developed by the interactions of the solid with the solvent and the molecules in solution, among other effects. In this figure, it is easy to see that the enthalpies of immersion in water are greater than the enthalpies of immersion in solutions, except for the 250 mg L^{-1} caffeine solution in SBA-15. This is evidence of endothermic processes present in the adsorption of both study molecules; so, energy produced by the interaction between the water molecule

https://doi.org/10.1021/acsomega.1c01588
ACS Omega 2021, 6, 21339−21349

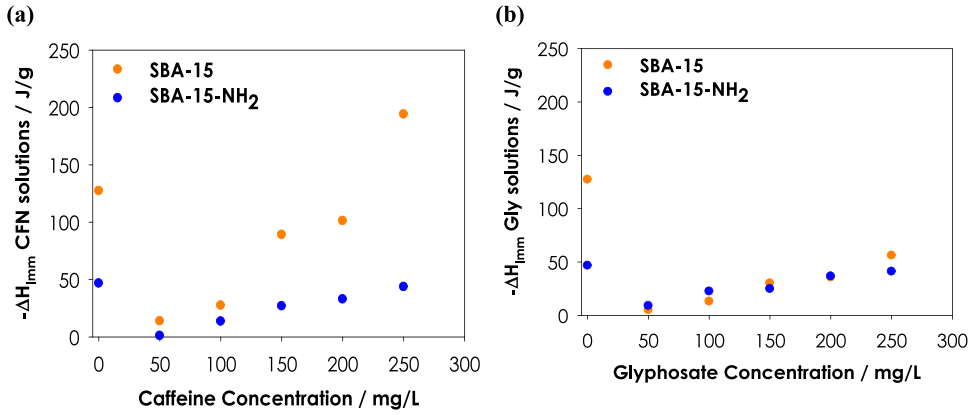

Figure 8. Enthalpy of immersion in solutions of (a) caffeine and (b) glyphosate of different concentrations (50−250 mg L^{-1}) on SBA-15 and SBA-15-NH_2.

Table 4. Parameter fits of Models of Langmuir, Freundlich, Redlich−Peterson, and Sips to Experimental Data of Caffeine Adsorption

caffeine								
two-parameter models								
	Langmuir model			Freundlich model				
sample	Q_o (mg g^{-1})	K_L (mL mg^{-1})	R^2	K_F (mL g^{-1})	$1/n$	R^2		
SBA-15	6.94	30.3	0.510	6.92	0.0003	0.510		
SBA-15-NH_2	4.45	0.029	0.856	0.4288	0.4609	0.860		
three-parameter models								
	Redlich−Peterson model				Sips Model			
sample	K_{RP} (mg g^{-1})	α_{RP} (mL mg^{-1})	β	R^2	Q_o (mg g^{-1})	K_S (mL mg^{-1})	$1/n_s$	R^2
SBA-15	4.84	0.424	1.14	0.510	18.6	6.32×10^{-7}	0.0449	0.509
SBA-15-NH_2	1.35	0.001	1.16	0.999	22.5	0.0004	0.5182	0.858

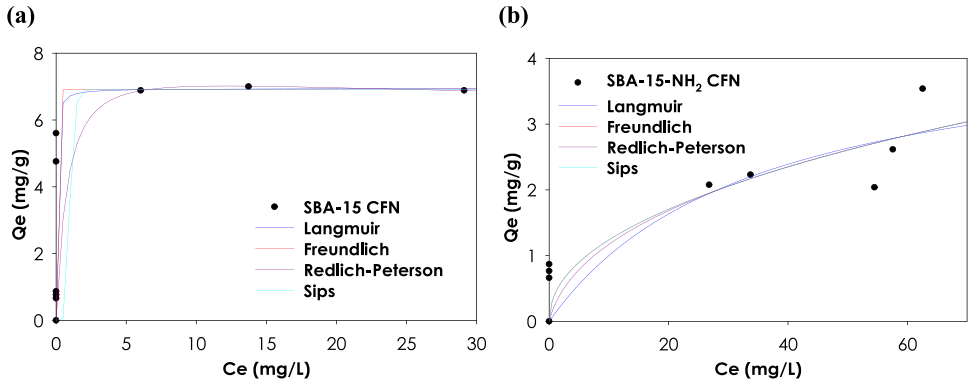

Figure 9. Caffeine adsorption isotherms of (a, b) SBA-15 and (c, d) SBA-15-NH_2.

(solvent) and active sites is used by molecules for the water molecule displacement and adsorption through the formation of specific and nonspecific interactions according to the chemistry of each molecule, as mentioned above (Figure 7).[43]

Critical molecular dimensions of caffeine and glyphosate are an important parameter to study the adsorption capacity and the interaction by solids with different textural parameters and mainly cylindrical geometry pores. According to Galhetas et al., the molecular dimensions of caffeine estimated by molecular modeling are 10.6 Å (length), 8.50 Å (width), and 4.50 Å (thickness).[44] Thus, according to the textural parameters evaluated for SBA-15 and SBA-15-NH_2 (summarized in Table 1), it is possible that there are restrictions to the diffusion of the caffeine molecule in the porous network of small dimensions (micropores) such as those that can be evaluated by the DR model, where an average pore width is between 8.03 and 10.5 Å for SBA-15 and SBA-15-NH_2, respectively, while in the mesoporous network, the half-pore width (Mode) evaluated by the DFT model has mainly pores with dimensions between 29.4 and 31.6 Å; that is to say, they are not restricted to the diffusion and adsorption of caffeine molecules.[45] However, according to Lima et al., the molecular dimensions of glyphosate have been estimated using molecular dynamics, and the distances between the centroids that minimize interaction potentials are 6.395, 7.410, and 8.220 Å.[46] So, in the same direction as in the previous analysis, it is possible that due to the molecular dimension of glyphosate, it is unlikely that there are restrictions on the diffusion of the glyphosate

https://doi.org/10.1021/acsomega.1c01588
ACS Omega 2021, 6, 21339−21349

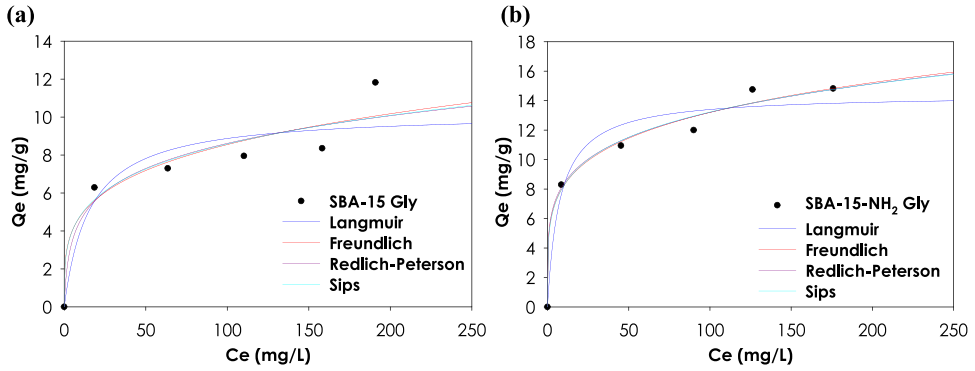

Figure 10. Glyphosate adsorption isotherms of (a) SBA-15 and (b) SBA-15-NH_2.

Table 5. Parameter Fits of Models of Langmuir, Freundlich, Redlich−Peterson, and Sips to Experimental Data of Glyphosate Adsorption

glyphosate								
two-parameter models								
	Langmuir model			Freundlich model				
sample	Q_o (mg g^{-1})	K_L (mL mg^{-1})	R^2	K_F (mL g^{-1})	$1/n$	R^2		
SBA-15	10.3	0.064	0.939	2.691	0.251	0.960		
SBA-15-NH_2	14.4	0.132	0.979	5.126	0.205	0.994		
three-parameter models								
	Redlich−Peterson model				Sips model			
sample	K_{RP} (mg g^{-1})	α_{RP} (mL mg^{-1})	β	R^2	Q_o (mg g^{-1})	K_S (mL mg^{-1})	$1/n_s$	R^2
SBA-15	2.509	0.721	0.796	0.957	49.31	0.056	0.288	0.959
SBA-15-NH_2	388.8	73.10	0.803	0.994	70.84	0.075	0.242	0.994

molecule in the mesoporous network. However, it could appear in the micropores formed in the walls (Table 4).

Silica samples obtained were tested as adsorbents of caffeine and glyphosate from aqueous solutions. The adsorption isotherms were measured by varying the initial concentration in a range between 50 and 250 mg L^{-1}, and the initial pH was not adjusted. The caffeine and glyphosate isotherms on the SBA-15 and SBA-15-NH_2 samples are presented in Figures 9a,b and 10a,b. The amount of caffeine and glyphosate adsorbed on the surface of the silica studied and the initial concentrations of caffeine in solutions increased.

The isotherms on SBA-15 have a pronounced initial slope that indicates a high efficiency of the material at low concentration; the adsorption capacity increases due to the gradual occupation of the active adsorption sites until the saturation of the adsorbent is complete. As described above, the effect of the increase in the driving force by the concentration gradient on the dynamic equilibrium of adsorption can be observed for each of the concentrations studied.[47] Ptaszkowska-Koniarz et al. analyzed the same behavior and claim that at low caffeine concentrations, the process of adsorption is totally random because there are many sites available for adsorption; however, when the caffeine concentration increases, they can be packed in the pore network.[48] The oxygen functional groups of SBA-15, silanol groups, can form hydrogen bonds with the basic nitrogen and oxygen atoms in caffeine since these organic molecules are aromatic and can donate π electrons.

The isotherm of caffeine onto SBA-15-NH_2 is of S type according to Giles classification;[49] this form of the isotherm is associated with the energy of adsorption, which is dependent on the solution concentration and the competitive effect between solvent molecules and caffeine molecules by the same active sites. Also, the water molecules can hydrate the caffeine molecule and block the interaction groups, and this effect is known as steric hindrance. As the concentration of caffeine increases, the adsorption occurs more readily. As mentioned earlier, there is a synergistic effect with the adsorbed molecules by establishing adsorbate−adsorbate interactions, or cooperative adsorption. In the last section of the isotherm, an increase in the adsorption capacity is observed due to a reorientation of the adsorbed molecules in the direction of a denser packing.

Higher caffeine adsorption capacity by SBA-15 can be related to the porous structure of the adsorbent, i.e., the larger surface available for adsorption and the high concentration of mesopore channels, which allow the connection between mesopores and micropores in the structure. The chemical nature of amino groups in SBA-15-NH_2, which are Lewis bases, could increase the available active sites for the interaction with caffeine through hydrogen-bonding interaction. It would be expected that these mechanisms are favored in the functionalization process; however, the sample SBA-15-NH_2 presents a low capacity of adsorption and calorimetric effect. The decrease of the removal can be attributed to the decrease of the textural parameters and therefore a lower disposition of the porosity for the adsorption process given by a steric impediment by the anchoring of bulky molecules such as APTES.

Figure 10a,b shows the isotherms for glyphosate adsorption on SAB-15 and SBA-15-NH_2, respectively. Glyphosate removal can be associated with both the textural and chemical characteristics of SBA-15, which suggests the suitability of this type of adsorbent for the elimination of this pesticide. The volume and diameter of the pores allow rapid diffusion kinetics

https://doi.org/10.1021/acsomega.1c01588
ACS Omega 2021, 6, 21339−21349

of glyphosate within the pore structure. Furthermore, the adsorption interaction between glyphosate and SBA-15-NH_2 is expected to take place through interaction with protonated amino groups through ion exchange and chelation mechanisms and the negatively charged functionalities of the herbicide.[50,51]

Later, to optimize the characterization of the adsorption systems, appropriate correlation of the experimental equilibrium points was established. For this reason, the Langmuir, Freundlich, Redlich−Peterson, and Sips models were used to describe the nature of the adsorption equilibrium. The adjustment parameters of the models are calculated by the quasi-Newton Rosenbrock optimization method included in the STATISTICA software and are summarized in Table 5. The abovementioned sorption isotherm models can be expressed by the following equations

$$\text{Langmuir} \quad Q_e = \frac{Q_0 K_l C_e}{1 + K_l C_e} \tag{3}$$

$$\text{Freundlich} \quad Q_e = K_F C_e^{1/n} \tag{4}$$

$$\text{Redlich} - \text{Peterson} \quad Q_e = \frac{K_{RP} C_e^{\beta}}{1 + \alpha_{RP} C_e^{\beta}} \tag{5}$$

$$\text{Sips} \quad Q_e = \frac{Q_0 K_s C_e^{1/n_s}}{1 + K_s C_e^{1/n_s}} \tag{6}$$

Comparison of the above four isotherm models evaluated by the use of correlation coefficient (R^2) values suggests that the Redlich−Peterson model is the best for SBA-NH_2, while for SBA-15, there are no differences between the models employed. Redlich−Peterson isotherm combines Langmuir and Freundlich isotherm characteristics.[52] This proposes that the adsorption capacity of caffeine onto SBA-15-NH_2 was induced by surface heterogeneity of the adsorbent.

Considering the Q_o parameter of the Langmuir model for caffeine adsorption, 6.94 and 4.45 mg g^{-1} for SBA-15 and SBA-15-NH_2, respectively, it is evident that these values were higher than those reported for SBA-15 and SBA-15 modified with Co^{2+}, Ni^{2+}, or Cu^{2+}(Q_o = 0.23, 0.07, 0.01, and 0.08 mg g^{-1}, respectively).[53] However, the values found in this research were lower compared to other adsorbents and conditions such as Q_o = 155.50 mg g^{-1} onto activated carbon fibers prepared from pineapple plant leaves,[54] Q_o = 118.0 and 107.0 mg g^{-1} on carbon xerogel modified with $(CH_3COO)_2Cu$ and ethylene diamine and carbon xerogel modified with $(CH_3COO)_2Cu$, respectively,[48] Q_o = 182.5 mg g^{-1} onto carbon xerogel treated with urea solution,[55] Q_o = 126.0 mg g^{-1} on activated carbon oxidized with HNO_3,[5656] Q_o = 190.9 mg g^{-1} onto activated carbon,[57] and, in addition, maximum adsorption capacities were 89.2, 129.6, and 916.7 mg g^{-1} for grape stalk, grape stalk modified by phosphoric acid, and activated carbon from grape stalk, respectively.[45]

For the process of glyphosate adsorption on the silicas, the Sips model better predicts the behavior of the adsorption of glyphosate molecules with correlation coefficients, $R^2 > 0.99$. This model predicted higher adsorption capacities for SBA-15-NH_2 (70.84 mg g^{-1}, see Table 4), related to the heterogeneity of the surface, n_s is the parameter of the Sips model, which shows the degree of surface nonhomogeneity.[58] Along with Redlich−Peterson isotherm, the Sips isotherm is a product of the combination of the Langmuir and Freundlich isotherms, and it can be used to predict the heterogeneous systems and hybrid adsorption mechanisms. It has also been shown to respond to changes in adsorbate concentrations, pH, and temperature of the study system. The values of n_s obtained for the Sips equation were between 3.47 and 4.13, indicating that the Sips isotherms tend to fit the Freundlich model, suggesting that the adsorption of glyphosate occurs in mono−multilayers on the surface of SBA-15 and SBA-15-NH_2. On the other hand, K_S is related to the sorption affinity between glyphosate and active sites on the surface;[59] this parameter is higher for SBA-15-NH_2.

3. CONCLUSIONS

The enthalpies of the study systems (whose values are between −5.06 and −194.06 J g^{-1}) describe an adsorption process that involves a process energetically higher than ion exchange (chemical interaction). It is considered that the establishment of specific interactions determines the adsorption capacity of the solids. The evidence of the attachment of the amino groups by FTIR, N_2 adsorption−desorption, and immersion calorimetry was confirmed. SBA-15-NH_2 exhibited an enhanced adsorption capacity provided by the establishment of new adsorption mechanisms, including amino groups. The anchorage of the APTES molecules for the modification of the surface of SBA-15 was verified by the changes in the IR spectra. A decrease in the intensity of the absorption band of the silanol groups was observed (located at 3400 cm^{-1}) and the presence of characteristic bands associated with primary amines at 1600 cm^{-1} and propyl groups between 2870 and 2940 cm^{-1}.

The experimental data of the equilibrium adsorption were fitted to the Langmuir, Freundlich, Redlich−Peterson, and Sips models. Three-parameter models were more appropriate to predict the behavior of caffeine and glyphosate adsorption, showing a hybrid adsorption mechanism.

4. MATERIALS AND METHODS

4.1. Porous Solids. The method followed for the synthesis of SBA-15 is known as the sol−gel method, using Pluronic, P123 (Aldrich, poly(ethylene oxide)−poly(propylene oxide)−poly(ethylene oxide); MW 5800), as the structuring agent, while silica source is from tetraethyl orthosilicate (TEOS), 98% Aldrich. The procedure was as follows: 18 g of pluronic P123 was added to 135 g of water and kept under constant stirring for 2 h. After that, it was transferred to a double-walled glass reactor at 35 °C and then 450 mL of 2 M HCl solution was added. Once the structuring agent was dissolved, the silica source (TEOS) was added drop by drop. The mixture was kept under constant stirring for 24 h. Then, the reaction temperature was raised to 80 °C for 24 h. The obtained solid was recovered by filtration under vacuum and was washed with deionized water several times until no foam appears. Finally, the solid was calcined at 540 °C for 6 h.[60] For the functionalization process by grafting of the (3-aminopropyl) triethoxysilane (APTES) molecule, 2 g of SBA-15 was mixed with 5 g of APTES in 100 mL of ethanol; this mixture was taken to boiling point in a glass reflux system. After 3 h, the mixture was filtered and the solid was washed three times with ethanol. Finally, the solid was placed on an oven at 80 °C for 12 h; this solid is named SBA-15-NH_2.[6161]

4.2. Physicochemical Characterization. Textural parameters, such as apparent surface area, pore volume, and average

https://doi.org/10.1021/acsomega.1c01588
ACS Omega 2021, 6, 21339−21349

half-pore width of silica solids, were evaluated by N_2 adsorption at −196 °C in a semiautomatic sortometer, IQ2 Autosorb of Quantachrome Instruments. Brunauer−Emmett−Teller (BET), Dubinin−Radushkevich (DR), Barrett−Joyner−Halenda (BJH) methods and diffusion functional theory (DFT) models were applied to determine the surface area, half-pore width, and pore size distribution (PSD). The thermal stability of the solids was studied by thermogravimetric analysis using a TA instrument (STA 7200Q HITACHI). Approximately 20 mg of the solid was placed in a crucible, the equipment was programmed to a heating ramp of 5 °C min^{-1} up to a maximum of 700 °C, and the experiment was carried out under a helium atmosphere (flow: 100 mL min^{-1}). From the registered weight loss and the differential, thermogravimetric curves were obtained. Additionally, the macrostructure of the solids were observed using a scanning electron microscope (SEM). SEM micrographs were obtained using a JEOL 6490-LV microscope and dry sample was placed on a metal surface for maximum contrast in the micrographs. The sample was then shifted to the SEM chamber and was observed at an accelerating voltage of 5 kV at different magnifications (1000−10 000×). Finally, the nature and changes in the surface chemistry were studied by FTIR spectroscopy. IR spectra were obtained using a Shimadzu FTIR spectrophotometer. The sample was pulverized and diluted in KBr.[62,63]

4.3. Determination of Caffeine Immersion Enthalpy and Adsorption Capacity from Aqueous Solutions. Caffeine solutions were prepared with Caffeine (Merck, analytical grade reagent) and doubly distilled water. The concentration range used for the study of adsorption was between 50 and 250 mg L^{-1}. These were prepared by dilution from stock solution (1000 mg L^{-1}). The reading of the calibration curve and solution isotherms were carried out in a UV−vis spectrophotometer (Thermo Spectronic Genesys 5) at 273 nm. Glyphosate solutions were prepared from Roundup herbicide and doubly distilled water at the same concentrations mentioned above. The UV−vis detection method used was that developed by Bhaskara and Nagaraja by reacting ninhydrin in the presence of sodium molybdate for the formation of the Ruhemann purple complex, which has a maximum absorbance at 570 nm.[64]

Immersion calorimetry experiments were performed using a Calvet-type heat conduction calorimeter. Wetting liquids used for the calorimetric characterizations were water and caffeine and glyphosate solutions with concentrations between 50 and 250 mg L^{-1}. To determine the immersion enthalpies, ∼0.080 g of the solid was weighed into a fragile-peak glass ampoule, while 8 mL of water was discharged into the calorimeter cell; then the calorimeter was assembled and the potential was recorded. Once thermal equilibrium was achieved (stable baseline), an aliquot of a concentrated caffeine solution was added to obtain the required concentration (50−250 mg L^{-1}) and the resulting effect was recorded until the stable baseline was obtained again. Recordings were then continued for an additional 10 min, followed by electrical calibration of the calorimeter. Experiments were repeated between three and four times for each solution until a deviation of less than 2% was obtained.[65−67]

Finally, the solids were tested for the adsorption of caffeine and glyphosate from aqueous solution. Caffeine and glyphosate solutions with concentrations between 50 and 250 mg L^{-1} were prepared, and 5 mL of each solution of caffeine was placed in a 20 mL flask. Then, 0.050 g of solid was added to the solution. The mixtures were kept at 25 °C with constant stirring for 24 h until equilibrium was reached. At the end of this equilibration time, the mixture was filtered through 0.45 μm poly(tetrafluoroethylene) (PTFE) syringes to remove the solid and the residual concentrations were determined by UV−vis spectroscopy. The experimental data of the adsorption isotherms from an aqueous phase were adjusted to the Langmuir, Freundlich, Redlich−Peterson, and Sips models.

AUTHOR INFORMATION

Corresponding Author

Juan Carlos Moreno-Piraján − *Departamento de Química, Facultad de Ciencias, Universidad de los Andes, 111711 Bogotá, Colombia*; Email: jumoreno@uniandes.edu.co

Authors

Paola Rodríguez-Estupiñan − *Departamento de Química, Facultad de Ciencias, Universidad de los Andes, 111711 Bogotá, Colombia*

Yaned Milena Correa-Navarro − *Departamento de Química, Facultad de Ciencias, Universidad de los Andes, 111711 Bogotá, Colombia; Departamento de Química, Facultad de Ciencias, Universidad de Caldas, 170002 Manizales, Colombia*

Diana P. Vargas − *Departamento de Química, Grupo de Investigación en Materiales Porosos con Aplicaciones Tecnológicas y Ambientales, Facultad de Ciencias, Universidad del Tolima, 730006299 Ibagué, Colombia*

Liliana Giraldo − *Departamento de Química, Facultad de Ciencias, Universidad Nacional de Colombia, 111321 Bogotá, Colombia*

Complete contact information is available at: https://pubs.acs.org/10.1021/acsomega.1c01588

Notes

The authors declare no competing financial interest.

ACKNOWLEDGMENTS

The authors thank the Faculty of Ciencias of Universidad de los Andes for the partial funding through the project INV-2018-33-1283 and Universidad de Caldas for the support to doctoral studies. The authors also wish to express their gratitude to the Ministry of Science and Technology of Colombia (Minciencias) and its Call 811-2018 "Postdoctoral stay program for MINCIENCIAS training beneficiaries in SNCTeI entities". Prof. Dr. Juan Carlos Moreno-Piraján also appreciates the financial support granted through research project number INV-2019-91-1905, for Vicerector for Research of the Universidad de los Andes.

REFERENCES

(1) Basheer, A. A. New generation nano-adsorbents for the removal of emerging contaminants in water. *J. Mol. Liq.* **2018**, *261*, 583−593.

(2) Mansour, F.; Al-Hindi, M.; Yahfoufi, R.; Ayoub, G.; Ahmad, M. N. The use of activated carbon for the removal of pharmaceuticals from aqueous solutions: a review. *Rev. Environ. Sci. Bio/Technol.* **2018**, *17*, 109−145.

(3) Ighalo, J. O.; Adeniyia, A. G.; Adelodun, A. A. Recent advances on the adsorption of herbicides and pesticides from polluted waters: Performance evaluation via physical attributes. *J. Ind. Eng. Chem.* **2021**, *93*, 117−137.

(4) Pal, A.; He, Y.; Jekel, M.; Reinhard, M.; Gin, K. Emerging contaminants of public health significance as water quality indicator compounds in the urban water cycle. *Environ. Int.* **2014**, *71*, 46−62.
(5) Tran, N. H.; Reinhard, M.; Gin, K. Y. H. Occurrence and fate of emerging contaminants in municipal wastewater treatment plants from different geographical regions-a review. *Water Res.* **2018**, *133*, 182−207.
(6) Álvarez-Torrellas, S.; Rodríguez, A.; Ovejero, G.; Gómez, J. M.; García, J. Removal of caffeine from pharmaceutical wastewater by adsorption: Influence of NOM, textural and chemical properties of the adsorbent. *Environ. Technol.* **2016**, *37*, 1618−1630.
(7) Divisekara, T.; Navaratne, A. N.; Abeysekara, A. S. K. Impact of a commercial glyphosate formulation on adsorption of Cd(II) and Pb(II) ions on paddy soil. *Chemosphere* **2018**, *198*, 334−341.
(8) De Andrade, J. R.; Oliveira, M. F.; Da Silva, M. G. C.; Vieira, M. G. A. Adsorption of Pharmaceuticals from Water and Wastewater Using Nonconventional Low-Cost Materials: A Review. *Ind. Eng. Chem. Res.* **2018**, *57*, 3103−3127.
(9) Rosenholm, J. M.; Czuryszkiewicz, T.; Kleitz, F.; Rosenholm, J. B.; Lindén, M. On the Nature of the Brønsted Acidic Groups on Native and Functionalized Mesoporous Siliceous SBA-15 as Studied by Benzylamine Adsorption from Solution. *Langmuir* **2007**, *23*, 4315−4323.
(10) Verma, P.; Kuwahara, Y.; Mori, K.; Raja, R.; Yamashita, H. Functionalized mesoporous SBA-15 silica: recent trends and catalytic applications. *Nanoscale* **2020**, *12*, 11333−11363.
(11) Moon, H.; Han, S.; Scott, S. L. Tuning molecular adsorption in SBA-15-type periodic mesoporous organosilicas by systematic variation of their surface polarity. *Chem. Sci.* **2020**, *11*, 3702−3712.
(12) Thielemann, F. G.; Schlögl, R.; Hess, C. Pore structure and surface area of silica SBA-15: influence of washing and scale-up. *Beilstein J. Nanotechnol.* **2011**, *2*, 110−118.
(13) Prestianggi, Y.; Maylisa, N.; Subagyono, R.; Sitorus, D. Adsorption of toluene and xylene from aqueous solution on SBA-15 from rice. *J. Phys.: Conf. Ser.* **2019**, *1277*, No. 012002.
(14) Liou, T.-H.; Liou, Y. H. Utilization of Rice Husk Ash in the Preparation of Graphene-OxideBased Mesoporous Nanocomposites with Excellent Adsorption Performance. *Materials* **2021**, *14*, No. 1214.
(15) Miricioiu, M.; Niculescu, V. C.; Filote, C.; Raboaca, M. S.; Nechifor, G. Coal Fly Ash Derived Silica Nanomaterial for MMMs—Application in CO2/CH4 Separation. *Membranes* **2021**, *11*, No. 78.
(16) Abid, Z.; Hakiki, A.; Boukoussa, B.; Launay, F.; Hamaizi, H.; Bengueddach, A.; Hamacha, R. Preparation of highly hydrophilic PVA/SBA-15 composite materials and their adsorption behavior toward cationic dye: effect of PVA content. *J. Mater. Sci.* **2019**, *54*, 679−769.
(17) Zhai, Q-Z.; Li, X-D. Efficient removal of cadmium(II) with SBA-15 nanoporous silica: studies on equilibrium, isotherm, kinetics and thermodynamics. *Appl. Water Sci.* **2019**, *9*, No. 143.
(18) Kim, H-J.; Yang, H-C.; Chung, D-Y.; Yang, I-H.; Choi, Y.; Moon, J-K. Functionalized Mesoporous Silica Membranes for CO2 Separation Applications. *J. Chem.* **2015**, *2015*, No. 202867.
(19) Zhang, Y.; Song, J.; Quispe Mayta, J.; Pan, F.; Gao, X.; Li, M.; Song, Y.; Wang, M.; Cao, X.; Jiang, Z. Enhanced desulfurization performance of hybrid membranes using embedded hierarchical porous SBA-15. *Front. Chem. Sci. Eng.* **2020**, *14*, 661−672.
(20) Vavsari, V. F.; Ziarani, G. M.; Badieic, A. The role of SBA-15 in drug delivery. *RSC Adv.* **2015**, *5*, 91686−91707.
(21) Albayati, T. M.; Salih, I. K.; Alazzawi, H. F. Synthesis and characterization of a modified surface of SBA-15 mesoporous silica for a chloramphenicol drug delivery system. *Heliyon* **2019**, *5*, No. e02539.
(22) Paul, L.; Mukherjee, S.; Chatterjee, S.; Bhaumik, A.; Das, D. Organically Functionalized Mesoporous SBA-15 Type Material Bearing Fluorescent Sites for Selective Detection of HgII from Aqueous Medium. *ACS Omega* **2019**, *4*, 17857−17863.
(23) Hasanzadeh, M.; Shadjou, N.; Guardia, M.; Eskandani, M.; Sheikhzadeh, P. Mesoporous silica-based materials for use in biosensors. *TrAC, Trends Anal. Chem.* **2012**, *33*, 117−129.
(24) Sweta, V. C. Synthesis and catalytic activity of SBA-15 supported catalysts for styrene oxidation. *Chin. J. Chem. Eng.* **2018**, *26*, 1300−1306.
(25) Akopyan, A.; Polikarpova, P.; Gul, O.; Anisimov, A.; Karakhanov, E. Catalysts Based on Acidic SBA-15 for Deep Oxidative Desulfurization of Model Fuels. *Energy Fuels* **2020**, *34*, 14611−14619.
(26) Rodríguez-Estupiñán, P.; Giraldo, L.; Moreno-Piraján, J. C. Calorimetric study of amino-functionalised SBA-15. *J. Therm. Anal. Calorim.* **2015**, *121*, 127−134.
(27) Madani, S. H.; Silvestre-Albero, A.; Biggs, M. J. Immersion Calorimetry: Molecular Packing Effects in Micropores. *ChemPhysChem.* **2015**, *16*, 3984−3991.
(28) Kjellman, T.; Asahina, S.; Schmitt, J.; Impéror-Clerc, M.; Terasaki, O.; Alfredsson, V. Direct observation of plugs and intrawall pores in SBA-15 using low voltage high resolution scanning electron microscopy and the influence of solvent properties on plug-formation. *Chem. Mater.* **2013**, *20*, 4105−4112.
(29) Thommes, M.; Kaneko, K.; Neimark, A. V.; Olivier, J. P.; Rodriguez-Reinoso, F.; Rouquerol, J.; Sing, K. S. W. Physisorption of gases, with special reference to the evaluation of surface area and pore size distribution (IUPAC Technical Report). *Pure Appl. Chem.* **2015**, *87*, 1051−1069.
(30) Guillet-Nicolas, R.; Ahmad, R.; Cychosz, K. A.; Kleitz, F.; Thommes, M. Insights into the pore structure of KIT-6 and SBA-15 ordered mesoporous silica-recent advances by combining physical adsorption with mercury porosimetry. *New J. Chem.* **2016**, *40*, 4351−4360.
(31) Ojeda, M. L.; Esparza, J. M.; Campero, A.; Cordero, S.; Kornhausera, I.; Rojas, F. On comparing BJH and NLDFT pore-size distributions determined from N2 sorption on SBA-15 substrata. *ChemPhysChem* **2003**, *5*, 1859−1866.
(32) Zhang, F.; Meng, Y.; Gu, D.; Chen, Z.; Tu, B.; Zhao, D. An aqueous cooperative assembly route to synthesize ordered mesoporous carbons with controlled structures and morphology. *Chem. Mater.* **2006**, *22*, 5279−5288.
(33) Landers, J.; Gor, G. Y.; Neimark, A. V. Density functional theory methods for characterization of porous materials. *Colloids Surf., A* **2013**, *437*, 3−32.
(34) Monson, P. A. Understanding adsorption/desorption hysteresis for fluids in mesoporous materials using simple molecular models and classical density functional theory. *Microporous Mesoporous Mater.* **2012**, *160*, 47−66.
(35) Ojeda-López, R.; Pérez-Hermosillo, I. J.; Esparza-Schulz, J. M.; Cervantes-Uribe, A.; Domínguez-Ortiz, A. SBA-15 materials: calcination temperature influence on textural properties and total silanol ratio. *Adsorption* **2015**, *8*, 659−669.
(36) Kim, S.; Park, S.; Han, Y.; Choi, J.; Park, J. Adsorption of Co(II) and Mn(II) Ions on Mesoporous Silica SBA15 Functionalized with Amine Groups. *Mater. Trans.* **2014**, *9*, 1494−1499.
(37) Kozlova, S. A.; Kirik, S. Post-synthetic activation of silanol covering in the mesostructured silicate materials MCM-41 and SBA-15. *Microporous Mesoporous Mater.* **2010**, *133*, 124−133.
(38) Bocian, S.; Rychlicki, G.; Matyska, M.; Pesek, J.; Buszewski, B. Study of hydration process on silica hydride surfaces by microcalorimetry and water adsorption. *J. Colloid Interface Sci.* **2014**, *416*, 161−166.
(39) Rodríguez-Estupiñán, P.; Bastidas-Barranco, M. J.; Moreno-Piraján, J. C.; Giraldo, L. A comparison of the energetic interactions in the adsorption of Co(II) from aqueous solution on SBA-15 and chemically modified activated carbons. *Adsorption* **2015**, *21*, 623−632.
(40) Yamamoto, K.; Shiono, T.; Yoshimura, R.; Matsui, Y.; Yoneda, M. Influence of hydrophilicity on adsorption of caffeine onto montmorillonite. *Adsorpt. Sci. Technol.* **2018**, *36*, 967−981.
(41) Liédana, N.; Marín, E.; Téllez, C.; Coronas, J. One-step encapsulation of caffeine in SBA-15 type and non-ordered Silicas. *Chem. Eng. J.* **2013**, *223*, 714−721.
(42) Arroyave, J.; Waiman, C.; Zanini, G.; Avena, M. Effect of humic acid on the adsorption/desorption behavior of glyphosate on goethite. Isotherms and kinetics. *Chemosphere* **2016**, *145*, 34−41.

https://doi.org/10.1021/acsomega.1c01588
ACS Omega 2021, 6, 21339−21349

(43) Carvajal-Bernal, A. M.; Gómez-Granados, F.; Giraldo, L.; Moreno-Piraján, J. C. A study of the interactions of activated carbon-phenol in aqueous solution using the determination of immersion enthalpy. *Appl. Sci.* **2018**, *8*, No. 843.
(44) Galhetas, M.; Mestre, A. S.; Pinto, M. L.; Gulyurtlu, I.; Lopes, H.; Carvalho, A. P. Chars from gasification of coal and pine activated with K2CO3: Acetaminophen and caffeine adsorption from aqueous solutions. *J. Colloid Interface Sci.* **2014**, *433*, 94−103.
(45) Portinho, R.; Zanella, O.; Féris, L. A. Grape stalk application for caffeine removal through adsorption. *J. Environ. Manage.* **2017**, *202*, 178−187.
(46) Lima, J.D.M.; Gomes, D. S.; Frazao, N. F.; Soares, D. J. B.; Sarmento, R. G. Glyphosate adsorption on C60 fullerene in aqueous medium for water reservoir depollution. *J. Mol. Model.* **2020**, *26*, No. 110.
(47) Srivastava, V. C.; Mall, I. D.; Mishra, I. M. Competitive adsorption of cadmium (II) and nickel (II) metal ions from aqueous solution onto rice husk ash. *Chem. Eng. Process.* **2009**, *48*, 370−379.
(48) Ptaszkowska-Koniarz, M.; Goscianska, J.; Pietrzak, R. Synthesis of carbon xerogels modified with amine groups and copper for efficient adsorption of caffeine. *Chem. Eng. J.* **2018**, *345*, 13−21.
(49) Giles, C. H.; MacEwan, T. H.; Nakhwa, S. N.; Smith, D. Studies in Adsorption: Part XI. A System of Classification of Solution Adsorption Isotherms and Its Use in Diagnosis of Adsorption Mechanisms and in Measurement of Specific Surface Area Solids. *J. Chem. Soc.* **1960**, *14*, 3973−3993.
(50) Rivoira, L.; Appendini, M.; Fiorilli, S.; Onida, B.; Del Bubba, M.; Bruzzoniti, M. C. Functionalized iron oxide/SBA-15 sorbent: investigation of adsorption performance towards glyphosate herbicide. *Environ. Sci. Pollut. Res.* **2016**, *23*, 21682−21691.
(51) Fiorilli, S.; Rivoira, L.; Calì, G.; Appendini, M.; Bruzzoniti, M. C.; Coïsson, M.; Onida, B. Iron oxide inside SBA-15 modified with amino groups as reusable adsorbent for highly efficient removal of glyphosate from water. *Appl. Surf. Sci.* **2017**, *411*, 457−465.
(52) Redlich, O.; Peterson, D. L. A useful adsorption isotherm. *J. Am. Chem. Soc.* **1958**, *63*, 1024−1025.
(53) Ortiz-Martínez, K.; Guerrero-Medina, K. J.; Román, F. R.; Hernández-Maldonado, A. J. Transition metal modified mesoporous silica adsorbents with zero microporosity for the adsorption of contaminants of emerging concern (CECs) from aqueous solutions. *Chem. Eng. J.* **2015**, *264*, 152−164.
(54) Beltrame, K. K.; Cazetta, A. L.; de Souza, P. S. C.; Spessato, L.; Silva, T. L.; Almeida, V. C. Adsorption of caffeine on mesoporous activated carbon fibers prepared from pineapple plant leaves. *Ecotoxicol. Environ. Saf.* **2018**, *147*, 64−71.
(55) Álvarez, S.; Ribeiro, R. S.; Gomes, H. T.; Sotelo, J. L.; García, J. Synthesis of carbon xerogels and their application in adsorption studies of caffeine and diclofenac as emerging contaminants. *Chem. Eng. Res. Des.* **2014**, *5*, 229−238.
(56) Torrellas, S. A.; García-Lovera, R.; Escalona, N.; Sepúlveda, C.; Sotelo, J. L.; García, J. Chemical-activated carbons from peach stones for the adsorption of emerging contaminants in aqueous solutions. *Chem. Eng. J.* **2015**, *279*, 788−798.
(57) Sotelo, J. L.; Ovejero, G.; Rodríguez, A.; Álvarez, S.; Galán, J.; García, J. Competitive adsorption studies of caffeine and diclofenac aqueous solutions by activated carbon. *Chem. Eng. J.* **2014**, *240*, 443−453.
(58) Hassan, V.; Hamidreza, H.; Hamidreza, B. Experimental and modeling investigation of adsorption equilibrium of CH4, CO2, and N2 on activated carbon and prediction of multi-component adsorption equilibrium. *Fluid Phase Equilib.* **2020**, *508*, No. 112433.
(59) Sodagar, A.; Ebrahimnejad, P.; Heydarinasab, A.; Akbarzadeh, A. Adsorption and controlled release of iron-chelating drug from the amino-terminated PAMAM/ordered mesoporous silica hybrid materials. *J. Drug Delivery Sci. Technol.* **2020**, *56*, No. 101579.
(60) Zhao, D.; Feng, J.; Huo, Q.; Melosh, N.; Fredrickson, G. H.; Chmelka, B. F.; Stucky, G. D. Triblock copolymer syntheses of mesoporous silica with periodic 50 to 300 angstrom pores. *Science* **1998**, *279*, 548−552.
(61) Northcott, K.; Kokusen, H.; Komatsu, Y.; Stevens, G. Synthesis and Surface Modification of Mesoporous Silicate SBA-15 for the Adsorption of Metal Ions. *Sep. Sci. Technol.* **2006**, *41*, 1829−1840.
(62) Rodríguez-Reinoso, F.; Molina-Sabio, M. Textural and chemical characterization of microporous carbons. *Adv. Colloid Interface Sci.* **1998**, *76*−*77*, 271−294.
(63) Szymański, G. S.; Karpiński, Z.; Biniak, S.; Świątkowski, A. The effect of the gradual thermal decomposition of surface oxygen species on the chemical and catalytic properties of oxidized activated carbon. *Carbon* **2002**, *40*, 2627−2639.
(64) Bhaskara, B. L.; Nagaraja, P. Direct Sensitive Spectrophotometric Determination of Glyphosate by Using Ninhydrin as a Chromogenic Reagent in Formulations and Environmental Water Samples. *Helv. Chim. Acta* **2006**, *89*, 2686−2693.
(65) Stoeckli, F.; Centeno, T. A. On the characterization of microporous carbons by immersion calorimetry alone. *Carbon* **1997**, *35*, 1097−1100.
(66) Giraldo, L.; Moreno-Piraján, J. C. Immersion enthalpy variation of surface-modified mineral activated carbon in lead (II) aqueous solution adsorption: The relation between immersion enthalpy and adsorption capacity. *Ecletica Quim.* **2006**, *31*, 15−21.
(67) Denoyel, R.; Rouquerol, F.; Rouquerol, J. Porous Texture and Surface Characterization from Liquid-Solid Interactions Immersion Calorimetry and Adsorption from Solution. In *Adsorption by Carbons*, 1st ed.; Bottani, E. J.; Tascón, J. M. D., Eds.; Elsevier Ltd: Netherlands, 2008; pp 273−300.

https://doi.org/10.1021/acsomega.1c01588
ACS Omega 2021, 6, 21339−21349